THE JOURNAL OF PHYSICAL CHEMISTRY C

Article

pubs.acs.org/JPCC

First-Principles Study of Crown Ether and Crown Ether-Li Complex Interactions with Graphene

Wei-Hua Wang,[†,‡] Cheng Gong,[†] Weichao Wang,[†,‡] Susan K. Fullerton-Shirey,[§] Alan Seabaugh,[§] and Kyeongjae Cho*[,†]

[†]Department of Materials Science and Engineering, The University of Texas at Dallas, 800 West Campbell Road, Richardson, Texas 75080, United States

[‡]Department of Electronics & Tianjin Key Laboratory of Photo-Electronic Thin Film Device and Technology, College of Electronic Information and Optical Engineering, Nankai University, 94 Weijin Road, Nankai District, Tianjin 300071, P. R. China

[§]Department of Electrical Engineering, University of Notre Dame, 275 Fitzpatrick Hall, Notre Dame, Indiana 46556, United States

Supporting Information

ABSTRACT: Adsorption of molecules on graphene is a promising route to achieve novel functionalizations, which can lead to new devices. Density functional theory is used to calculate stabilities, electronic structures, charge transfer, and work function for a crown-4 ether (CE) molecule and a CE−Li (or CE−Li^+) complex adsorbed on graphene. For a single CE on graphene, the adsorption distance is large with small adsorption energies, regardless of the relative lateral location of the CE. Because CE interacts weakly with graphene, the charge transfer between the CE and graphene is negligibly small. When Li and Li^+ are incorporated, the adsorption energies significantly increase. Simultaneously, an *n*-type doping of graphene is introduced by a considerable amount of charge transfer in CE−Li adsorbed system. In all of the investigated systems, the linear dispersion of the p_z band in graphene at the Dirac point is well-preserved; however, the work function of graphene is effectively modulated in the range of 3.69 to 5.09 eV due to the charge transfer and the charge redistribution by the adsorption of CE−Li and CE−Li^+ (or CE), respectively. These results provide graphene doping and work function modulation without compromising graphene's intrinsic electronic property for device applications using CE-based complexes.

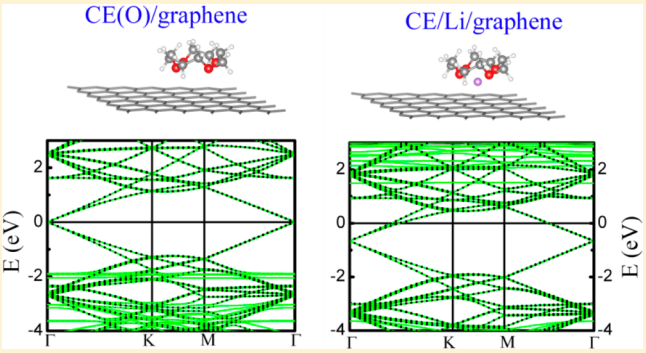

1. INTRODUCTION

Graphene has attracted extensive research interest due to its superior electronic properties and potential application in nanoelectronics, nanoionics, chemical sensors, and other fields.[1−4] Its low-energy physics process can be depicted by the linear band dispersion in the vicinity of the Dirac point, which makes the carriers behave like massless Dirac Fermions.[1] Consequently, ultrahigh intrinsic carrier mobility of 2×10^5 $cm^2/(V\ s)$[5] and room-temperature ballistic transport properties[6] are demonstrated. Pristine graphene can be regarded as a semiconductor with zero band gap or a semimetal with vanishing density of states (DOS) at the Fermi level. The absence of a band gap is an impediment to use of graphene for logic applications because the graphene field-effect transistor does not turn off well. Graphene functionalization, however, has been an important research topic. An energy gap can be induced by forming nanoribbons,[7] by graphene hydrogenation,[8−10] or by applying a vertical electric field.[11,12] Unfortunately, the linear band structure is usually destroyed and the carrier mobility shrinks dramatically using these approaches. Moreover, in most graphene-based sensor devices, it is desired to modulate the carrier concentration of graphene by shifting the Fermi level away from the Dirac point. This can be realized by noncovalent interaction with adsorbates, making the adsorption of molecules on graphene a promising route to achieve an effective doping;[13,14] however, a high doping level in some cases is not easily obtained due to the weak interaction and the small amount of charge transfer between the molecule and graphene.[13] Thus, it is desirable to explore a doping strategy that increases the binding strength between the adsorbate and the graphene and simultaneously offers control of both sheet carrier density and work function.

Crown ethers (CEs) are macrocyclic molecules with the chemical formula $(CH_2CH_2O)_n$, where the number of monomer units, *n*, determines the cavity size of the molecule. One property of CEs is the site-selective binding with alkali ions,[15,16] making CE−cation complexes promising candidates for doping graphene. The advantage of this doping strategy is

Received: July 21, 2015
Revised: August 11, 2015
Published: August 11, 2015

DOI: 10.1021/acs.jpcc.5b07049
J. Phys. Chem. C 2015, 119, 20016−20022

that for certain values of n all of the O atoms in the CE−cation complexes will reside in the same plane, making possible the use of CE-cation complexes as a 2D dopant for graphene. For example, when the cation is Li^+ or Na^+, an O planar structure is formed for n = 4 and 5.[17]

From the viewpoint of graphene functionalization, the adsorption of CE−Li on graphene has several advantages over individual CE or Li adsorption. Compared with an isolated CE molecule, the introduction of Li is expected to increase the binding strength between CE and graphene, thereby increasing the stability and the effectiveness of the dopant. An increased binding energy has been reported between graphene and H_2 and free radicals when Li is coadsorbed.[18−20] Compared with the adsorption of only adatom Li on graphene,[2,21,22] the stability of the CE−Li complex on graphene should be higher due to the strong binding between CE and Li atoms and ions. As previously shown in the literature,[2,22] the lateral diffusion barrier of Li adatoms on perfect graphene is only ∼0.30 to 0.35 eV, indicating that Li is highly mobile on the graphene surface and will form clusters of bulk lithium. Lee et al.[23] and Das et al.[24] have shown that the adsorption of Li as the bulk metal phase on perfect graphene is energetically unfavorable. Thus, it is anticipated that the CE stabilizes the Li, preventing lateral Li diffusion because of the strong interaction strength between CE and Li. Considering these potential advantages, it is worth investigating the interaction of 2D CEs and CE−cation complexes with graphene and their influence on the electronic structure.

In this work, we choose to study the interaction between graphene and a CE−Li complex where n = 4, because it is the smallest CE with planar O atoms in the crown ether-cation complex. This adsorbate on graphene is referred to as CE, CE−Li, and CE−Li^+ for the remainder of the document, where Li is an atom in CE−Li and an ion in CE−Li^+. The stability, geometrical structure, charge transfer, electronic structure, and work function of the CE and CE−Li complex adsorbed on graphene are investigated by density functional theory (DFT) calculations. Our data show that the improvement of the binding strength of the CE with graphene and an effective n-type doping are both achieved by the introduction of Li in CE−Li adsorbed on graphene. Regardless of the presence of Li in the CE, the adsorption does not impact the linear dispersion of the p_z bands. The charge transfer results in an upward shift of the Fermi level away from the Dirac point by ∼0.67 eV, which reduces the work function of the graphene. Although the charge transfer is minor in CE and CE−Li^+ adsorbed systems, the electric dipole formation owing to the charge redistribution modulates the work function of graphene significantly. These theoretical results provide insights into the applications of nanoelectronics and nanoionics utilizing graphene functionalization with CE molecules and alkali metals.

2. COMPUTATIONAL MODEL AND DETAILS

All calculations are performed by Vienna ab initio Simulation Package (VASP)[25,26] with projected augmented wave (PAW) pseudopotentials.[27] After testing different exchange-correlation potentials (see Figure S1a), the local density approximation (LDA)[28] has better accounted the interaction between adsorbate and graphene, and it is adopted for the study because it can produce a negative adsorption energy and a similar equilibrium adsorption distance. The electron wave function is expanded in the plane wave basis set with an energy cutoff of 450 eV. The Γ-centered Monkhorst−Pack k-point grid in the irreducible Brillouin zone (BZ) sampling is used by 3 × 3 × 1 for the structural relaxation and by 9 × 9 × 1 for the subsequent self-consistent electronic calculation. The atomic structure optimization stops when the force acting on each atom is <0.03 eV/Å. The converged energy criterion is 10^{-5} eV in the calculation of electronic properties. To acquire an accurate charge density, 160 × 160 × 218 fast Fourier transformation (FFT) meshes are adopted in real space.

In the hexagonal primitive unit cell of graphene, two C atoms are arranged in a 2D honeycomb lattice with an optimized lattice constant of 2.46 Å. To accurately study one CE and one CE−Li complex interaction with graphene, the dependence of adsorption energy on the supercell size is systematically explored. (See Figure S1b.) The 6 × 6 graphene supercell with 72 C atoms is determined to be a reasonably accurate supercell size, and it is adopted throughout this paper. As shown in Figure 1, three different adsorption configurations are

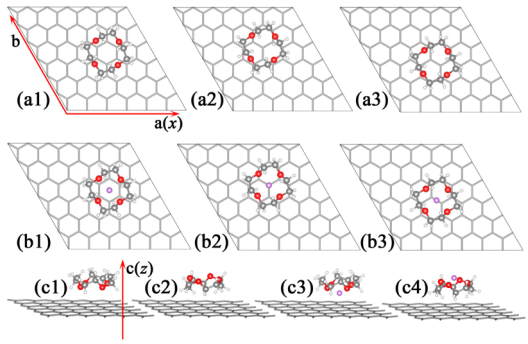

Figure 1. Top views of different configurations for CE on single-layer graphene with (a1) C (center) site, (a2) T (top) site, and (a3) B (bridge) site and CE−Li(or Li^+) complex on single-layer graphene with (b1) C site, (b2) T site, and (b3) B site. (c1−c4) Side views of CE(O)/graphene, CE(H)/graphene, CE/Li(or Li^+)/graphene, and Li(or Li^+)/CE/graphene. The gray, red, white, and purple spheres represent the C atom, O atom, H atom, and Li atom, respectively. The graphene layer is displayed by the gray sticks.

defined based on either the relative position of the center of mass for four O atoms in the CE or the Li in CE−Li complex to that of the C atoms in graphene. The three configurations correspond to the center (C) site in Figure 1a1,b1, the top (T) site in Figure 1a2,b2, and the bridge (B) site in Figure 1a3,b3. Side views of the systems in two contact configurations are shown for CE (Figure 1c1,c2) and CE−Li (Figure 1c3,c4) adsorbed on graphene. In Figure 1c1,c3, the O side of the CE is facing the graphene, while it is facing away from the graphene in Figure 1c2,c4. For simplicity, the graphene lattice is aligned with x−y plane, and the z axis is normal to the graphene plane. To minimize the interaction between periodic images, a 20 Å lattice constant is used in the z direction. For each configuration, in one adsorbed system, the CE in all directions, the Li along the z axis, and the C atoms of graphene in x−y plane are fully relaxed until the most energetically favorable structure is reached. The supercell volume is fixed during all relaxations. We have tested the effect of also relaxing the C atoms of graphene in the z direction, and the maximum deviation of C in the z position from the graphene layer is <0.02 Å. Thus, the distortion of graphene in the z direction can be ignored, which is similar to that of other organic molecular systems adsorbed on graphene.[13] For CE−Li^+ adsorbed on graphene, one electron is removed from the system. Mean-

DOI: 10.1021/acs.jpcc.5b07049
J. Phys. Chem. C 2015, 119, 20016−20022

Table 1. Adsorption Energy (E_{ad}) and Structural Parameters for (a) an Isolated CE Molecule or Li atom and (b) CE−Li Adsorbed on Graphene with Three Configurations (Center (C), Top (T), and Bridge (B) Site)[a]

(a)

system	E_{ad} (eV)	ΔE (eV)	d_{O-G} in CE/graphene or d_{Li-G} in Li/graphene (Å)
CE(O)/graphene	C −0.532	0.000	2.993
	T −0.528	0.004	2.932
	B −0.515	0.017	2.997
CE(H)/graphene	C −0.444	0.038	4.333
	T −0.482	0.000	4.316
	B −0.462	0.020	4.323
Li/graphene	C −1.946	0.000	1.667
	T −1.588	0.358	1.965
	B −1.622	0.324	1.892

(b)

system	E_{ad} (eV)	ΔE (eV)	d_{O-G} (Å)	d_{Li-G} (Å)	d_{O-Li} (Å)
CE/Li/graphene	C −2.796	0.000	3.019	2.134	0.885
	T −2.781	0.015	3.152	2.236	0.916
	B −2.760	0.036	3.052	2.238	0.814
Li/CE/graphene	C −2.860	0.033	4.216	4.815	0.599
	T −2.893	0.000	4.194	4.802	0.608
	B −2.836	0.057	4.225	4.837	0.612
CE/Li^+/graphene	C −2.242	0.009	3.052	2.253	0.799
	T −2.251	0.000	3.024	2.313	0.711
	B −2.232	0.019	3.073	2.326	0.747
Li^+/CE/graphene	C −2.180	0.030	4.305	4.976	0.671
	T −2.210	0.000	4.315	4.983	0.668
	B −2.169	0.041	4.351	5.016	0.665

[a]Stability of different configurations is indicated by the energy difference between the adsorption energy of some specific state and that of the lowest energy state. The structure parameters of the distance from O plane in CE to graphene layer (d_{O-G}), that from Li to graphene layer (d_{Li-G}), and that between Li and O plane (d_{O-Li}) are also listed.

while, an additional negative background charge is applied to neutralize the system in VASP to avoid the Coulomb divergence issue. A larger 8 × 8 supercell (19.68 Å × 19.68 Å in *xy* plane) with 20 Å thickness in *z* axis is also tested to estimate the effect of negative background charge on the energy calculations. The difference in the adsorption energy is <0.05 eV between 6 × 6 and 8 × 8 supercells, indicating the small effect for 6 × 6 supercell systems.

3. RESULTS AND DISCUSSION

To study the stability of adsorbed structures, the adsorption energy of the adsorbate on graphene is calculated based on the formula

$$E_{ad} = E_{graphene+adsorbate} - E_{graphene} - E_{adsorbate} \quad (1)$$

where $E_{graphene+adsorbate}$, $E_{graphene}$, and $E_{adsorbate}$ represent the total energy of the relaxed adsorbate with graphene, the energy of the 6 × 6 pristine graphene, and the energy of the adsorbate, respectively. The adsorbate is defined as one CE molecule, Li atom, or CE−Li complex.

Because the CE is asymmetric along the plane defined by the O atoms, two contact configurations exist. One is the O side of the molecule facing the graphene, and the other where the H side facing the graphene. As shown in Figure 1, the two different configurations based on the O side contact and H side contact with graphene are labeled by CE(O)/graphene and CE(H)/graphene in the following text. Table 1a summarizes the adsorption energy, E_{ad}, and the distance between the O plane in CE and graphene, d_{O-G}. It is found that the C site configuration is the most stable for the CE(O)/graphene system with the adsorption energy −0.532 eV and the equilibrium distance, d_{O-G}, of 2.993 Å. Interestingly, although the T-site and B-site configurations are slightly unfavorable compared with the C site structure, the difference in adsorption energy among these three configurations is only 17 meV, and d_{O-G} is ∼3.0 Å in all cases. This means that lateral diffusion of the CE molecule on graphene may be favorable, similar to the organic molecule, tetrathiafulvalene (TTF), on graphene.[13] The minor energy difference among the configurations results from the large distance between CE and graphene and the weak interaction between them. In contrast with the CE(O)/graphene system, for CE(H)/graphene system, the T-site configuration has the largest adsorption energy, −0.482 eV, and d_{O-G} is 4.316 Å. Similar to the CE(O)/graphene system, the variation of adsorption energies for all three structures is also small (∼38 meV). When comparing the two systems, the O side contact configuration is slightly more stable than that of H side contact. The energy difference of −50 meV is due to the stronger interaction between O and C than H and C. The adsorption energies and stable distances from Li to the graphene plane, d_{Li-G}, for an isolated Li atom adsorbed on graphene (Li/graphene) are also listed in Table 1a to provide easy comparison with the CE−Li/graphene systems. The Li atom prefers to bind at the C site with graphene, and the binding distance is 1.667 Å. The energy barrier for Li moving from one stable C site to another through a T site in between is ∼0.36 eV. Our data on Li/graphene system are in agreement with the literature.[18,29]

Likewise, there also exist two contact configurations when Li is introduced in CE/graphene system. Because Li prefers to bind to the O side of the CE, the two configurations are labeled

DOI: 10.1021/acs.jpcc.5b07049
J. Phys. Chem. C 2015, 119, 20016−20022

as CE/Li/graphene (Figure 1c3) and Li/CE/graphene (Figure 1c4). As shown in Table 1b, the C site configuration is energetically favorable for the former system, whereas the T site is the most favorable for the latter. The type of stable configuration (i.e., C and T) is the same as that of a single CE adsorbed on graphene except for an additional Li atom; however, the adsorption energy is enhanced by a factor of ∼5 in the CE/Li/graphene system compared with the CE/graphene system, even though the distance between CE and graphene changes by <1%. It means that the presence of Li improves the binding interaction between CE and graphene. This is similar to the observation that the binding strength between graphene and H_2 or free radicals can be increased by Li coadsorption.[18−20]

Unlike the individual CE adsorbed on graphene, the Li/CE/graphene system is more stable by −0.097 eV than CE/Li/graphene system. To understand the variation of adsorption energy for both contact configurations induced by the presence of Li, the distance of Li relative to the O plane in CE, d_{O-Li}, is also listed in Table 1b. By examining the atomic structures, it is found that d_{O-Li} is 0.608 Å in Li/CE/graphene and d_{O-Li} is 0.885 Å in CE/Li/graphene. The shorter distance in Li/CE/graphene indicates a stronger binding interaction between the Li and the CE. Consequently, the total energy in Li/CE/graphene is reduced lower than in CE/Li/graphene. Compared with the CE/graphene system, the increase in the adsorption energy in CE−Li^+ complex adsorbed on graphene system is also observed. The T-site configuration is energetically favorable for both contact configurations; however, the stability among the three configurations and two adsorption configurations varies less than that of CE−Li atom system. For charged CE−Li^+ system, the energy correction (E_{corr}) issue induced by the spurious electrostatic interaction between periodic images is not serious because the supercell size we adopted is large enough. Referring to E_{corr} in MoS_2 with charged native defects,[29] the E_{corr} in CE−Li^+ adsorbed on graphene is estimated to be ∼0.05 eV.

To further examine and analyze the effect of Li on the interaction of CE with graphene, we use the formula as well

$$E_{ad} = E_{graphene+(CE-Li)} - E_{graphene+Li} - E_{CE} \quad (2)$$

to calculate the adsorption energy of CE with Li/graphene in the CE/Li/graphene system. This is similar to the approach described in ref 19 but where the hydrogen is replaced with the CE. Using eq 2, the adsorption energy is about −2.527 eV, which is larger than that of CE/graphene, −0.532 eV, similar to what is previously described. Such an increase in the adsorption energy in CE/Li/graphene relative to CE/graphene could be described by both eqs 1 and 2. Here we focus on the interaction between adsorbate (an isolated CE molecule and a CE−Li complex) with graphene; therefore, we adopt eq 1 in this work. The energy reference is taken as that from the isolated graphene and the adsorbate. Similarly, the adsorption of Li on pure graphene is also stabilized by incorporating the CE molecule. Compared with an isolated Li adsorbed on graphene,[2,30] the equilibrium distance (d_{Li-G} = 2.134 Å) from Li to the graphene in a CE/Li/graphene system becomes larger than that in Li/graphene (d_{Li-G} = 1.667 Å), but the stability is strengthened due to a strong binding of CE−Li.[15] It is worth noting that the Li would not easily form a cluster because of the strong binding between CE and Li, even though the energy difference among different configurations is only ∼0.036 eV for CE/Li/graphene and 0.057 eV for Li/CE/graphene. Therefore, the CE−Li complex is more favorable as an adsorbed dopant to graphene from the perspective of stability. The doping effect on graphene can be captured by the electronic structure calculations described in the following text.

To analyze the impact of the CE and CE−Li complex on the electronic structure of graphene, the total density of states (DOS) and the partial DOS (PDOS) are plotted in Figure 2A,B, respectively. Compared with the pristine graphene, CE and CE−Li complex adsorption does not significantly affect the electronic structure of graphene, except for shifting the Fermi level upward in the CE−Li system (Figure 2A(c,d)). The additional states below the Fermi level mainly come from the contribution of the CE, while those above the Fermi level partially originate from Li and CE (Figure 2B). To observe the PDOS of Li clearly, we scaled the original data by a factor of 30 in Figure 2B. As shown in Figure 2B(c,d), the *n*-type doping character of graphene is demonstrated in the CE−Li adsorbed on graphene. The adsorption concentration, defined as the

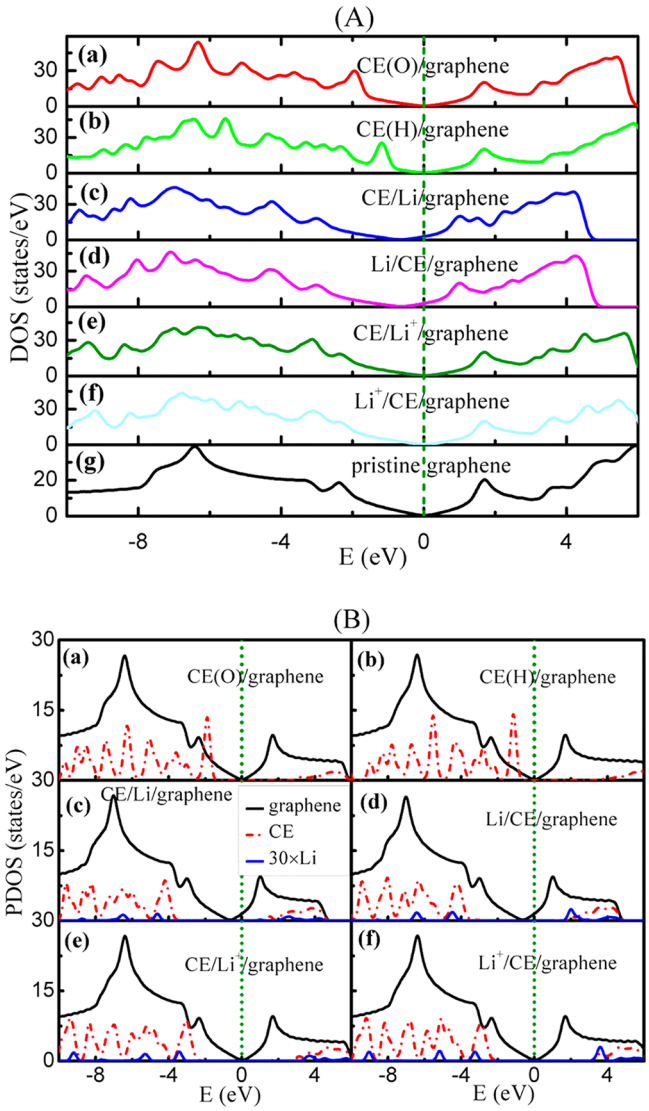

Figure 2. Total density of states (DOS) in (A) and partial DOS (PDOS) in (B) for (a) CE(O)/graphene, (b) CE(H)/graphene, (c) CE/Li/graphene, (d) Li/CE/graphene, (e) CE/Li^+/graphene, and (f) Li^+/CE/graphene. For comparison, the DOS of pristine graphene is plotted in (g) of panel A. The vertical dashed line is the Fermi level.

DOI: 10.1021/acs.jpcc.5b07049
J. Phys. Chem. C 2015, 119, 20016−20022

number of CE−Li complexes divided by the number of C atoms in graphene, is only 1.389% (i.e., 1/72). Similar to pristine graphene, the PDOS of graphene for all adsorbed cases in Figure 2B exhibit the typical pseudogap state feature of graphene. The band structures further verify that the linear band dispersions of p_z orbitals from C atoms in graphene at the Dirac point do not change, which is highlighted by the filled black circles in Figure 3. All of the results for the electronic structure support the noncovalent interaction between adsorbates and graphene.

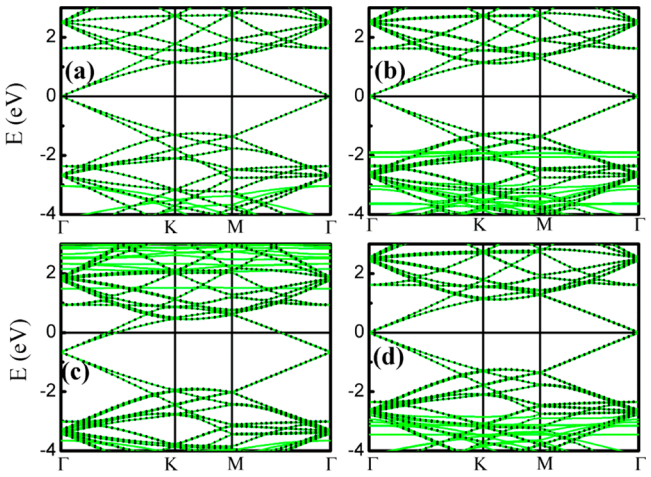

Figure 3. Band structures of (a) pristine graphene, (b) CE(O)/graphene, (c) CE/Li/graphene, and (d) CE/Li^+/graphene along the high symmetric directions in the first Brillouin zone. The Fermi level is set at zero energy. The contribution from the graphene carbon p_z orbital is highlighted by filled black circles.

So far we have found that the effective *n*-type doping of graphene can be induced even with a low concentration of the adsorbed CE−Li complex. At the same time, the Li atom clustering effect for only Li atoms adsorbed on graphene is also avoided by the binding of Li with CE. In previous studies of metal−graphene contact systems, the work function of the metal has a sizable effect on graphene.[31,32] In a similar way, the work function of graphene can be modulated considerably when the CE or CE−Li complex is adsorbed. Table 2 lists the charge state and the work function of graphene after charge transfer between the adsorbate and graphene. For the pristine graphene, the work function is 4.53 eV in our calculations, which is consistent with the experimental value of 4.57 ± 0.05 eV.[33] Because of the asymmetric geometry of the CE, the direction of the charge transfer and the change in the work function of graphene depends on which side of the CE is adsorbed on graphene: The work function decreases by 0.17 eV when the CE(O) side is in contact and it increases by 0.10 eV when the CE(H) side is in contact. The orientation of the CE molecule is also important when Li^+ is added: The graphene work function increases by 0.37 eV in the CE/Li^+/graphene system and by 0.56 eV in the Li^+/CE/graphene system; however, when Li is included in the system, the graphene work function decreases by ∼0.8 eV regardless of which side of the CE−Li complex adsorbed on graphene. It is noted that the charge state of Li is positive (∼1.1 e) in Li-involved systems, showing that the positive charge is nearly localized around Li. In other words, the removed electron in the supercell is primarily contributed by Li, which makes it suitable to simulate the Li^+ case.

Table 2. Charge State Based on Bader Charge Analysis and the Work Function (W) of Graphene in Six Adsorbed Systems[a]

system	charge state of graphene (e)	charge state of Li (e)	*W* (eV)
pristine graphene	0.0	N/A	4.53
CE(O)/graphene	0.016	N/A	4.36
CE(H)/graphene	−0.005	N/A	4.63
CE/Li/graphene	−0.891	1.122	3.69
Li/CE/graphene	−0.881	1.128	3.73
CE/Li^+/graphene	0.074	1.138	4.90
Li^+/CE/graphene	0.071	1.123	5.09

[a]For comparison, the pristine graphene work function is also provided.

The change of the work function is closely correlated with the charge transfer or the charge redistribution. Among all systems we investigated, a significant fraction of charge transfer occurs only in the systems where CE−Li is adsorbed on graphene. This mainly originates from the electron transfer from the Li to graphene sheet. The maximum of the electron doping density in graphene sheet (n_e) can be estimated from the charge state of graphene, −0.891 e in 6 × 6 system, where $n_e \approx 4.70 \times 10^{13}$ e/cm^2. An even higher doping density, by further reducing the supercell size, may be readily achieved as long as the stable adsorbed system is not affected by the strong interaction between the short-distance adsorbed complexes. In contrast, a lower doping density can be tuned by enlarging the supercell size, equivalently decreasing the adsorption concentration. The band structures, charge transfer, and the electron doping density are illustrated in Figure S2 and Table S1. In 6 × 6 system, the *n*-type doping to graphene can move up the Fermi level by ∼0.67 eV, deviating from the conical point, so the work function of graphene correspondingly decreases. More interestingly, even though the charge transfer is small in the other systems, changes in the graphene work function are still considerable. In fact, charge transfer is not the only factor that affects the work function of metals, as the interfacial dipole from the charge redistribution also plays a key role in some molecules or adatoms adsorbed on metal surfaces.[34,35] To understand the underlying mechanism of the change in the work function of graphene, we plot the *xy* plane averaged charge redistribution along the *z* axis in Figure 4. The difference charge density is defined as $\Delta\rho(z) = \rho_{G+CE(CE-Li)}(z) - \rho_G(z) - \rho_{CE(CE-Li)}(z)$, where the first term represents the charge density of the total system and the second and third terms are the charge density of the graphene layer and the CE or CE−Li complex, respectively. The charge accumulation or depletion close to the vacuum side of graphene is directly correlated to the decrease or increase in the work function of graphene, respectively. In detail, the charge accumulation facilitates the electron emission and lowers the work function in CE(O) or CE−Li adsorbed on graphene, as shown in Figure 4a,c. On the contrary, the charge depletion makes the electron emission more difficult, so the work function of graphene is enhanced in CE(H) or CE−Li^+ adsorbed on graphene systems in Figure 4b,d.

The charge redistribution arises from the chemical interaction between the adsorbate and the substrate. For instance, in an isolated CE adsorbed on graphene, the electronegativity of the O atom is stronger than that of the C atom, which leads to a small amount of electron transfer from

DOI: 10.1021/acs.jpcc.5b07049
J. Phys. Chem. C 2015, 119, 20016−20022

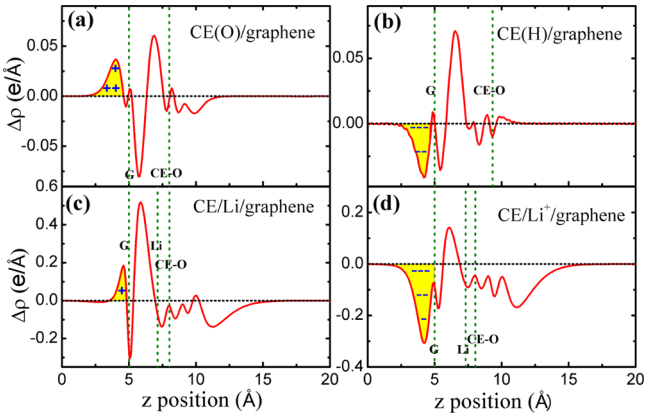

Figure 4. *xy* plane averaged difference charge density along *z* axis plots for (a) CE(O)/graphene, (b) CE(H)/graphene, (c) CE/Li/graphene, and (d) CE/Li^+/graphene. The positions of the graphene, O plane in CE, and Li are indicated by the vertical dashed lines. The shaded regions close to graphene surface indicate electron accumulation with "+" and depletion with "−".

graphene to CE in CE(O)/graphene. Besides the electron gain from graphene, the O atoms also receive electrons from C and H atoms inside the CE molecule, which induces electron accumulation at the O side of the CE. The electron−electron repulsion due to the Pauli Exclusion Principle drives the electrons in graphene away from the interface, accumulating close to the vacuum side of graphene in Figure 4a, which decreases the work function. Conversely, the H atoms with weaker electronegativity in CE(H)/graphene attract electrons in graphene, so the depletion region appears in the vacuum side of graphene and the work function of graphene increases in Figure 4b. In the CE−Li^+ adsorbed system, the charge accumulation region appears around the CE−Li^+ complex under the attraction of the positively charged Li^+, and thus the electron depletion region occurs close the vacuum side of graphene in Figure 4d, which results in the increased work function.

4. CONCLUSIONS

In summary, we have investigated the interactions of CE, CE−Li^+, and CE−Li adsorbed on pristine graphene by DFT calculations. The CE−Li adsorbate effectively introduces an *n*-type doping to graphene because of the charge transfer from Li to graphene. Furthermore, the change in the work function of graphene is significant in all adsorbed systems we have investigated due to the charge redistribution and charge transfer between the adsorbate and graphene. Our results provide a fundamental understanding and helpful guidance for graphene doping, work function control, and applications in nanoelectronics and nanoionics using CE-functionalized graphene.

■ ASSOCIATED CONTENT

Supporting Information

The Supporting Information is available free of charge on the ACS Publications website at DOI: 10.1021/acs.jpcc.5b07049.

Detailed calculations on different exchange-correlation potentials, different supercell sizes, and graphene electron doping density as a function of adsorption concentration. (PDF)

■ AUTHOR INFORMATION

Corresponding Author

*E-mail: kjcho@utdallas.edu. Tel: +01-972-883-2845.

Notes

The authors declare no competing financial interest.

■ ACKNOWLEDGMENTS

This work was supported in part by the Center for Low Energy Systems Technology (LEAST), one of six centers of STARnet, a Semiconductor Research Corporation program sponsored by MARCO and DARPA. W.-H.W. and W.W. also acknowledge the support from NSFC (nos. 11104148, 11404172, and 11304161). Parts of the calculations were performed at the Texas Advanced Computing Center (TACC) in Austin (http://www.tacc.utexas.edu).

■ REFERENCES

(1) Novoselov, K. S.; Geim, A. K.; Morozov, V.; Jiang, D.; Katsnelson, M. I.; Grigorieva, I. V.; Dubonos, S. V.; Firsov, A. A. Two-dimensional gas of massless Dirac fermions in graphene. *Nature (London, U. K.)* **2005**, *438*, 197−200.

(2) Chan, K. T.; Neaton, J. B.; Cohen, M. L. First-principles study of metal adatom adsorption on graphene. *Phys. Rev. B: Condens. Matter Mater. Phys.* **2008**, *77*, 235430/1−12.

(3) Georgakilas, V.; Otyepka, M.; Bourlinos, A. B.; Chandra, V.; Kim, N.; Kemp, K. C.; Hobza, P.; Zboril, R.; Kim, K. S. Functionalization of Graphene: Covalent and Non-Covalent Approaches, Derivatives and Applications. *Chem. Rev.* **2012**, *112*, 6156−6214.

(4) Boukhvalov, D. W.; Katsnelson, M. I. Chemical Functionalization of Graphene with Defects. *Nano Lett.* **2008**, *8*, 4373−4379.

(5) Morozov, S. V.; Novoselov, K. S.; Katsnelson, M. I.; Schedin, F.; Elias, D. C.; Jaszczak, J. A.; Geim, A. K. Giant Intrinsic Carrier Mobilities in Graphene and Its Bilayer. *Phys. Rev. Lett.* **2008**, *100*, 016602/1−4.

(6) Wu, J.; Becerril, H. A.; Bao, Z.; Liu, Z.; Chen, Y.; Peumans, P. Organic solar cells with solution-processed graphene transparent electrodes. *Appl. Phys. Lett.* **2008**, *92*, 263302/1−3.

(7) Yang, L.; Park, C. H.; Son, Y. W.; Cohen, M. L.; Louie, S. G. Quasiparticle Energies and Band Gaps in Graphene Nanoribbons. *Phys. Rev. Lett.* **2007**, *99*, 186801/1−4.

(8) Elias, D. C.; Nair, R. R.; Mohiuddin, T. M. G.; Morozov, S. V.; Blake, P.; Halsall, M. P.; Ferrari, A. C.; Boukhvalov, D. W.; Katsnelson, M. I.; Geim, A. K.; Novoselov, K. S. Control of Graphene's Properties by Reversible Hydrogenation: Evidence for Graphane. *Science* **2009**, *323*, 610−613.

(9) Sofo, J. O.; Chaudhari, A. S.; Barber, G. D. Graphane: A Two-Dimensional Hydrocarbon. *Phys. Rev. B: Condens. Matter Mater. Phys.* **2007**, *75*, 153401/1−4.

(10) Zhou, J.; Wu, M. W.; Zhou, X.; Sun, Q. Tuning electronic and magnetic properties of graphene by surface modification. *Appl. Phys. Lett.* **2009**, *95*, 103108/1−3.

(11) Zhang, Y. B.; Tang, T. T.; Girit, C.; Hao, Z.; Martin, M. C.; Zettl, A.; Crommie, M. F.; Shen, Y. R.; Wang, F. Direct Observation of a Widely Tunable Bandgap in Bilayer Graphene. *Nature (London, U. K.)* **2009**, *459*, 820−823.

(12) Castro, E. V.; Novoselov, K. S.; Morozov, S. V.; Peres, N. M. R.; Dos Santos, J.; Nilsson, J.; Guinea, F.; Geim, A. K.; Neto, A. H. C. Biased Bilayer Graphene: Semiconductor with a GapTunable by the Electric Field Effect. *Phys. Rev. Lett.* **2007**, *99*, 216802/1−4.

(13) Hu, T.; Gerber, I. C. Theoretical Study of the Interaction of Electron Donor and Acceptor Molecules with Graphene. *J. Phys. Chem. C* **2013**, *117*, 2411−2420.

(14) Wang, X.; Xu, J. B.; Xie, W.; Du, J. Quantitative Analysis of Graphene Doping by Organic Molecular Charge Transfer. *J. Phys. Chem. C* **2011**, *115*, 7596−7602.

(15) Datta, A. Role of Metal Ions (M) Li^+, Na^+, and K^+) and Pore Sizes (Crown-4, Crown-5, and Crown-6) on Linear and Nonlinear

DOI: 10.1021/acs.jpcc.5b07049
J. Phys. Chem. C 2015, 119, 20016−20022

Optical Properties: New Materials for Optical Birefringence. *J. Phys. Chem. C* **2009**, *113*, 3339−3344.
(16) Rodriguez, J. D.; Lisy, J. M. Probing Ionophore Selectivity in Argon-Tagged Hydrated Alkali Metal Ion Crown Ether Systems. *J. Am. Chem. Soc.* **2011**, *133*, 11136−11146.
(17) De, S.; Boda, A.; Ali, S. M. Preferential interation of charged alkali metal ions (guest) within a narrow cavity of cyclic crown ethers (neutral host): A quantum chemical investigation. *J. Mol. Struct.: THEOCHEM* **2010**, *941*, 90−101.
(18) Ataca, C.; Aktürk, E.; Ciraci, S.; Ustunel, H. High-capacity hydrogen storage by metallized graphene. *Appl. Phys. Lett.* **2008**, *93*, 043123/1−3.
(19) Liu, W.; Zhao, Y. H.; Nguyen, J.; Li, Y.; Jiang, Q.; Lavernia, E. J. Electric field induced reversible switch in hydrogen storage based on single-layer and bilayer graphemes. *Carbon* **2009**, *47*, 3452−3460.
(20) Denis, P. A. Chemical Reactivity of Lithium Doped Monolayer and Bilayer Graphene. *J. Phys. Chem. C* **2011**, *115*, 13392−13398.
(21) Fan, X.; Zheng, W. T.; Kuo, J.-L. Adsorption and Diffusion of Li on Pristine and Defective Graphene. *ACS Appl. Mater. Interfaces* **2012**, *4*, 2432−2438.
(22) Ishii, A.; Yamamoto, M.; Asano, H.; Fujiwara, K. DFT calculation for adatom adsorption on graphene sheet as a prototype of carbon nano tube functionalization. *Journal of Physics: Conference Series* **2008**, *100*, 052087/1−4.
(23) Lee, E.; Persson, K. A. Li Absorption and Intercalation in Single Layer Graphene and Few Layer Graphene by First Principles. *Nano Lett.* **2012**, *12*, 4624−4628.
(24) Das, D.; Kim, S.; Lee, K. R.; Singh, A. K. Li diffusion through doped and defected graphene. *Phys. Chem. Chem. Phys.* **2013**, *15*, 15128−15134.
(25) Kresse, G.; Hafner, J. *Ab initio* molecular dynamics for liquid metals. *Phys. Rev. B: Condens. Matter Mater. Phys.* **1993**, *47*, 558−561.
(26) Kresse, G.; Furthmüller, J. Efficiency of ab-initio total energy calculations for metals and semiconductors using a plane-wave basis set. *Comput. Mater. Sci.* **1996**, *6*, 15−50.
(27) Blochl, P. E. Projector augmented-wave method. *Phys. Rev. B: Condens. Matter Mater. Phys.* **1994**, *50*, 17953−17979.
(28) Ceperley, D. M.; Alder, B. J. Ground State of the Electron Gas by a Stochastic Method. *Phys. Rev. Lett.* **1980**, *45*, 566−569.
(29) Noh, J.-Y.; Kim, H.; Kim, Y.-S. Stability and electronic structures of native defects in single-layer MoS_2. *Phys. Rev. B: Condens. Matter Mater. Phys.* **2014**, *89*, 205417/1−12.
(30) Khantha, M.; Cordero, N. A.; Molina, L. M.; Alonso, J. A.; Girifalco, L. A. Interaction of lithium with graphene: An *ab initio* study. *Phys. Rev. B: Condens. Matter Mater. Phys.* **2004**, *70*, 125422/1−8.
(31) Giovannetti, G.; Khomyakov, P. A.; Brocks, G.; Karpan, V. M.; van den Brink, J.; Kelly, P. J. Doping Graphene with Metal Contacts. *Phys. Rev. Lett.* **2008**, *101*, 026803/1−4.
(32) Gong, C.; Lee, G.; Shan, B.; Vogel, E. M.; Wallace, R. M.; Cho, K. First-principles study of metal−graphene interfaces. *J. Appl. Phys.* **2010**, *108*, 123711/1−8.
(33) Yu, Y. J.; Zhao, Y.; Ryu, S.; Brus, L. E.; Kim, K. S.; Kim, P. Tuning the Graphene Work Function by Electric Field Effect. *Nano Lett.* **2009**, *9*, 3430−3434.
(34) Rusu, P. C.; Giovannetti, G.; Weijtens, C.; Coehoorn, R.; Brocks, G. Work Function Pinning at Metal-Organic Interfaces. *J. Phys. Chem. C* **2009**, *113*, 9974−9977.
(35) Black-Schaffer, A. M.; Cho, K. First-principles study of the work function of nitrogen doped molybdenum (110) surface. *J. Appl. Phys.* **2006**, *100*, 124902/1−4.

DOI: 10.1021/acs.jpcc.5b07049
J. Phys. Chem. C 2015, 119, 20016−20022